Elaboration and characterization of biocomposite based on polylactic acid and Moroccan sisal fiber as reinforcement

Zineb SAMOUH [1,2,3*], Kolos MOLNÁR[4,5], Sándor HAJBA[4], François BOUSSU[2] , Omar CHERKAOUI[3], Reddad EL MOZNINE[1]

[1]Laboratory LPMC. Faculty of Science El Jadida. Chouaib Doukkali University.M-24000 ElJadida. Morocco

[2]Laboratory GEMTEX. ENSAIT. University Lille North of France Centralelille. F-59100 Roubaix. France

[3]Laboratory REMTEX ESITH (Higher School of Textile and Clothing Industries). M- 20190Casablanca. Morocco

[4]Department of Polymer Engineering, Faculty of Mechanical Engineering, Budapest University of Technology and Economics. H-1111 Budapest. Hungary

[5]MTA–BME Research Group for Composite Science and Technology. Műegyetem rkp. 3., H-1111 Budapest, Hungary

*Corresponding author : zineb.samouh@gmail.com

Abstract:

The aim of the current study is to further investigate the impact of the sisal fiber content up to 30% on the mechanical and thermal properties of polylactic acid matrix composites following up to our previous study for sisal content up 15%. The biocomposites were prepared successfully using a twin-screw extruder and an injection molding machine. It was found that 20 m% resulted the best mechanical, dynamic mechanical and thermal properties among the tested fiber contents. Beyond this weight fraction of sisal these properties showed a slight decrease probably due to reaching the threshold percolation corresponding to weight fraction limit before the aggregations started to form in the matrix. This finding was supported by scanning electron microscopy. The degree of crystallinity increased until reaching 10% fiber content, but not above. The results revealed that the reinforcement of polylactic acid by sisal fiber does not only improve mechanical properties but also it could be used as a nucleating agent for the PLA. Moreover, a new relationship is proposed to characterize the effectiveness of the composite due to the addition of sisal fiber. The performance of the biocomposites developed makes them capable for applications in various fields such as aeronautics, automotive and construction.

Keywords: Composites; Natural fiber; Thermoplastics; Mechanical properties; Thermal properties.

1. INTRODUCTION

The composite materials offer several advantages including light weight, high strength, corrosion resistance and design flexibility [1]. The environmental concern has led scientists to

focus on a new generation of sustainable composite materials, so-called green composites. The conventional structural composite materials include synthetic fibers as reinforcement (glass fiber, carbon fiber; etc.) and non-biodegradable matrices such as epoxy resin, polyester resin, etc. [2]. However, the use of petroleum-based composite materials could have an environmental impact (climate change, pollution, greenhouse effect, difficult recycling). The advantages of natural fibers such as low cost, abundance, low density show the potential of these fibers for the replacement of synthetic fibers [3]. Natural fibers reinforcing composites may be obtained mainly from plants like hemp [4], bamboo [5], flax [6] and some from animal origin like silk [7] and wool [8].

Several studies were carried out to evaluate the performance of bio-based fibers and petroleum-based fiber reinforced composite materials [9-11]. Pickering et al. [12] reported that several factors (fiber selection, matrix selection, fiber separation and fiber orientation) affect the mechanical performance of composites materials. Various studies have been interested in introducing biodegradable polymers to develop biocomposites. The introduction of natural fibers into green composites has conducted scientists to evaluate the properties of the biopolymers with various natural fibers [13-14].

Several studies have focused on the influence of natural fiber content on the properties of biopolymers. The results reported by Lee. S. M et al. [15] show that the increase of novel silk up to 50 % in poly(butylene succinate) biocomposites provide good mechanical (tensile and flexural) properties such composites. Erika et al [16] proved that the increase of the agave fiber content up to 30 % improve the impact and flexural properties of polyhydroxybutyrate green composites . The fiber content is a factor influencing the mechanical performance and thermal stability of green composites. Arrakhiz et al. [17] evaluated the effect of doum fiber content on the thermal properties of low density polyethylene composites. The results show that adding 5% doum fiber to LDPE increased its enthalpy but above 5%, the enthalpy decreased continuously up to 30% (they did not measure it above 30%).

The mechanical performance and thermal stability of the polymer polylactic acid (PLA) shows the potential of this biopolymer in the development of biocomposites [18-19]. Several natural fibers have been used by researchers as a reinforcement of polylactic acid. Oksman et al. [20] show that the tensile strength of PLA composites with 30% flax fiber content was higher than the strength of PP composites with 30% flax fiber content. Placketta et al. [21] prove that 40 wt% jute fiber improved the stiffness of PLA. Gamon et al. found that an increase of miscan fiber content in polylactic (PLA) from 10% to 40% does not modify the glass transition temperature of the biopolymer [22]. Cheng et al. reported that the storage modulus of chicken feather fiber reinforced PLA increased as the weight fraction of chicken feather fibers was increased [23].

Sisal fiber is one of the most efficient natural fibers used for the reinforcement of polymers [24]: Polyethylene [25], Polypropylene [26-27]. Poly(hydroxybutyrate-co-valerate) (PHBV) [28]. In addition, the availability of sisal fiber in some countries is an important advantage and could provide the opportunity of using this fiber for the development of biocomposites.

In this context, the sisal fibers were selected as reinforcement to be used in a polylactic acid (PLA) matrix in view of the abundance of the Agave Sisalana plant in the north of Morocco [29]. This sisal fiber has only been used in traditional medicine in Morocco so far [30]. Our previous study focused on the development and characterization of green composites based on polylactic acid (PLA) with sisal fiber content from 0% to 15% [31]. The challenge of this work is to explore an abundant Moroccan natural resource to develop green composites with a high rate of reinforcement by studying the reinforcement efficiency of sisal fiber. The current study includes the development and characterization of biocomposites with a polylactic acid (PLA) matrix and up to 30% sisal fiber reinforcement (Scheme 1), and also the effect of the

reinforcement content of sisal fibers on the mechanical and thermal properties are presented and discussed.
Scheme 1. Development of biocomposites based on Moroccan sisal fibers

2. EXPERIMENTAL

2.1. Materials

The polylactic acid (Ingeo 3100HP) was obtained from Nature Works LLC. This polymer is biodegradable and highly biocompatible with good thermal properties (specific gravity 1.24 g/cm^3).
Sisal fibers are extracted mechanically from the leaves. The preparation of the fibers includes washing and drying. The preparation and behavior of sisal fibers used in the current study were reported in more detail in our previous study [31].

2.2. Preparation of biocomposites

The samples of biocomposites were produced by extrusion and injection molding. The matrix (PLA) was mixed with different weight fractions of sisal fibers (0%, 15%, 20%, 25% and 30%). In the following, we refer to these as pure PLA, PLA/15%SF, PLA/20%SF, PLA/25%SF, PLA/30%SF, respectively. The results for smaller fiber contents are taken from our previous **study [31].**
Then, the mixture (PLA and sisal fibers) was extruded with a Labtech LTE 26-44 twin-screw extruder (Labtech Engineering, Thailand). Based on the thermal properties of PLA (Ingeo 3100HP), the temperature of the extruder was 190 °C. The selected screw speed was 20 rpm. After extrusion, the obtained strands were cut into small pieces with a strand pelletizer (LZ-120). The specimens were produced with an Arburg Allrounder 270s (ARBURG Holding GmbH, Lossburg, Germany) injection molding machine. The temperature of the mold was 25 °C. Injection speed was 50 cm^3/s [31]. The dimension of the specimens is 170 mm x 10 mm x 4 mm.

2.3. Characterization of the biocomposites

2.3.1. Tensile Test
The tensile properties of the specimens were tested with a tensile tester (Zwick Z050 Zwick Roell, Germany) according to the ISO 527 standard. The crosshead speed was 5 mm/min. Five PLA composite specimens were tested for each reinforcement content at room temperature.

2.3.2. Flexural Test
The flexural properties of the samples were analyzed according to the ISO 178 standard. The method of flexural testing was three point bending. The flexural properties were measured at 21 °C with a crosshead speed of 2 mm/min (Zwick Z050 flexural tester, Zwick Roell, Germany).
Five samples were evaluated for each type of PLA biocomposite and compared to the five samples of pure matrix. The flexural strength (σ_{fM}) and flexural modulus (E_f) were calculated according to the following (1) and (2):

$$\sigma_{fM} = \frac{3FL}{2bh^2} \quad (1)$$

$$E_f = \frac{mL^3}{4bh^3} \quad (2)$$

where *F* is the maximum load (N), *L* is the length between the supports (mm), *m* is the slope of the initial linear part of the load–deformation curve, and *b* and *h* are width and depth, respectively [31].

2.3.3. Charpy impact test

The Charpy impact properties were investigated according to the ISO 179 standard. The composite specimens were tested with a Ceast Resil Impactor Junior test machine (CEAST, Italy). The Charpy impact analysis was performed at a room temperature (pendulum velocity: 2.9 m/s). Five specimens for each type of PLA biocomposite were evaluated and the average was calculated.

2.3.4. Differential scanning calorimetry (DSC)

The thermal properties were investigated with a Q2000 differential scanning calorimeter (TA Instruments, USA). The thermal analysis was carried out in three cycles (heat–cool–heat) between –30 and 200 °C. The rate of heating and cooling cycles was 5 °C/min and 10 °C/min, respectively. The degree of crystallinity (X_C) of the specimen was calculated according to (3):

$$X_C(\%) = \frac{\Delta H_m - \Delta H_{CC}}{\Delta H_{mo} * w} \cdot 100, \quad (3)$$

where ΔH_m and ΔH_{mo} are the melting enthalpies of PLA biocomposites and the 100% crystallinity of the chosen matrix (polylactic acid; 93.7 J/g [32]), respectively. ΔH_{cc} is the enthalpy of cold crystallization, and w is the weight fraction of PLA in the biocomposites.

2.3.5. Thermogravimetric Analysis (TGA)

The thermal stability of the biocomposites was studied with a universal thermogravimetric analyzer (Q500 of TA Instruments, USA). The thermal analysis was carried out with a heating range from 20 °C to 600 °C in nitrogen. The heating rate was 10 °C/min.

2.3.6. Dynamic Mechanical Analysis (DMA)

The dynamic mechanical properties of PLA biocomposites were investigated with a dynamic mechanical analyzer (Q800 of TA Instruments, USA) in three-point bending mode . The DMA tests were carried out from 20 °C up to 100 °C (heating rate: 5 °C/min, frequency: 1 Hz**, amplitude 15 µm**). The dimensions of the specimens of the composites was of 60 mm x 10 mm x 4 mm.

2.3.7. SEM microstructure of biocomposites

The surface morphology of PLA biocomposites were observed using a scanning electron microscope JEOL JSM 6380LA (Japan). The SEM images of the samples were processed with the Smile Shot™ software.

3. RESULTS AND DISCUSSION

3.1. Properties of sisal fiber

The average tensile strength of sisal fiber was 340.02±70.4MPa. The tensile modulus was **12.5 ± 7.8** GPa and the elongation at break was 3.2%. The density of sisal fiber was found to be 1.42 g/cm^3 and the diameter of sisal fiber was 239.0 ± 80.18 µm. More experimental details

on these properties were reported in our previous study [31]. It is well-known that the mechanical properties of sisal fibers strongly depend on their origin. These properties of sisal fiber used in the current study are reported in Table 1 as well as the mechanical properties of others sisal fibers from different places. The overall properties of the Moroccan sisal fibers seem to have good mechanical properties in comparison with other sisal fibers from different places.

Table 1 Comparison of the mechanical properties of sisal fibers from different countries

Fiber origin	Diameter (μm)	Tensile strength (MPa)	Young's modulus (GPa)	Elongation at break (%)	Reference
Morocco	*239.0±80.2*	*340.0±70.4*	*12.5±7.8*	*3.2±0.8*	*Current Study*
Indonesia	-	375.0±38.0	9.1±0.8	-	[39]
Mexico	-	283.5±12.10	5.24±14.7	7.84±10.98	[40]
Kenya	-	347.0±110.0	-	8.0±2.0	[41]
Brazil	200.0±75.6	391.0±89.0	10.7±4.0	5.2±2.5	[42]
India	269.8±78.0	294.0±113.0		-	[38]

3.2. Mechanical properties of biocomposites

3.2.1. Tensile properties

Figure 1 shows the tensile properties of PLA biocomposites. The improvement of the tensile properties of PLA biocomposites as a result of increasing sisal fiber content was investigated in two regions: in the first region, where the tensile strength of PLA biocomposites showed an increase with the addition of sisal fiber from 0% to 15%. In the second region, the tensile strength exhibited a slight increase from 15% to 20%, followed by a slight decrease between 20% and 30%.

In the first region, the tensile strength of PLA/15%SF and pure PLA are 135.1 ± 7.4 MPa and 109.6 ± 8.3MPa, respectively. Similar behavior was observed in our previous study [31]. The tensile strength was improved with an increase in the weight fraction of sisal fibers up 15% in PLA biocomposites. In the second region, tensile strength decreased because of the decohesion behavior between PLA and the sisal fibers, which contributes to stress concentration [33].

The tensile modulus was also enhanced with increasing sisal fiber content up to 30% in PLA biocomposites. The percentage of tensile modulus increment compared to that of pure PLA was 58.62%, 62%, 71.37% and 72.76%, with sisal fiber contents of 15%, 20%, 25% and 30%, respectively.

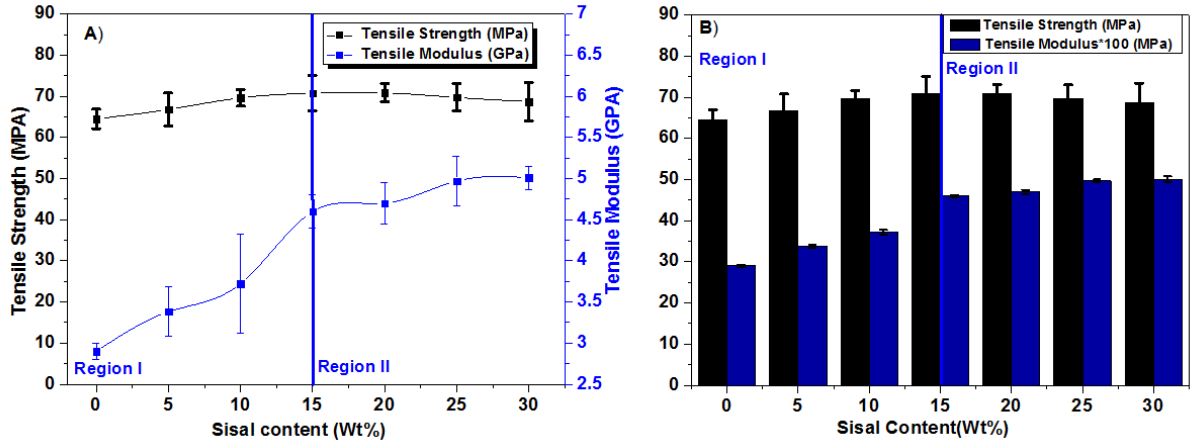

Figure 1 Tensile properties of the sisal fiber reinforced PLA biocomposites (a) Curves (b) Bar diagram

3.2.2. Flexural properties

Figure 2 (a) and (b) shows the flexural properties of PLA biocomposites. The flexural properties showed similar trends to tensile properties. The change of flexural properties also showed two regions: in the first region, flexural strength increased between 0% and 15% sisal fiber content. The flexural strength of PLA/15%SF and pure PLA was 135.1±7.4 MPa and 109.6 ± 8.3MPa, respectively. In the second region, flexural strength showed a slight increase between 15% and 20% and then decreased very slightly between 20% and 30%. The flexural strength of PLA composites with 15%, 20%, 25% and 30% sisal fiber content were 135.1±7.4 MPa, 136.5±9.3MPa, 135.4±10.6 MPa and 134.5±9.5MPa, respectively. The flexural strength of 30% sisal fiber reinforced PLA is 15% greater than the flexural strength of 30% wood reinforced composites [35]. The flexural strength of PLA biocomposites changed in the same way as the tensile strength of PLA biocomposites with increasing fiber content. The pineapple leaf fiber was used as reinforcement of polylactic acid in [36]. The flexural strength PLA composites with 20% untreated and treated pineapple leaf fiber was 57 MPa and 64 MPa, respectively [36]. The flexural strength of the PLA with 20% sisal fiber was 136.5±9.3 MPa in our study. Therefore, PLA–sisal fiber composites had better flexural properties than PLA/untreated pineapple leaf fiber and PLA/treated pineapple leaf fiber composites [36].

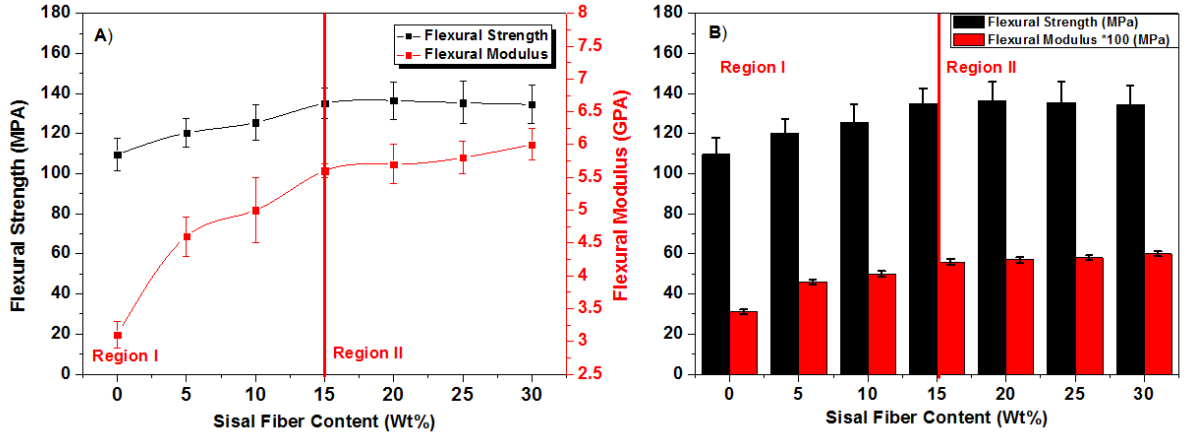

Figure 2 Flexural properties of sisal fiber-reinforced PLA biocomposites. (a) Curves (b) Bar diagram

3.2.3. Charpy impact properties

The Charpy impact properties of the PLA biocomposites were plotted in Figure 3 (a) and (b). Two regions can also be observed: The first is where Charpy impact strength increased up to 15% fiber content. In the second, the Charpy impact strength of PLA biocomposites was quite high at 20% fiber content. With more reinforcement, the Charpy impact strength of PLA biocomposites decreased. The Charpy impact strength of PLA/15%SF, PLA/20%SF, PLA/25%SF and PLA/30%SF is higher by 30.30%, 89.89%, 67.67% and 67%, respectively, than that of pure PLA. The impact strength of PLA/20%SF is higher than the impact strength of PLA/20% PLA/untreated pineapple leaf fiber and PLA/20%treated pineapple leaf fiber in the study carried out by Darsan. This decrease in impact strength of pineapple fiber reinforced PLA can be caused by voids and fiber pull-out in the composite [36].

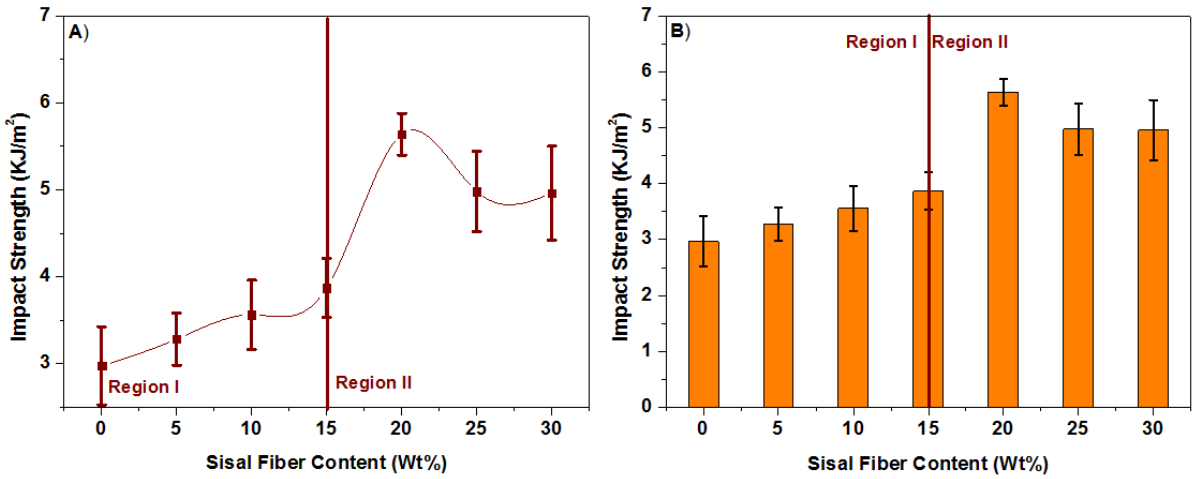

Figure 3 Impact properties of the sisal fiber-reinforced PLA biocomposites. (a) Curves (b) Histogram

The mechanical properties of sisal fiber–PLA biocomposites are summarized in Table 2. The results of the mechanical tests show that there is a significant, general improvement due to the addition of sisal fibers. The tensile modulus together with the flexural modulus continuously increases as the fiber content increases. The impact strength and the elongation at break has a local maximum at 20% sisal fiber content.

Therefore, in our opinion, a sisal fiber content of 20% is probably optimal for overall good mechanical properties. Higher fiber content might lead to compounding issues that hinders further improvement.

Table 2 Mechanical properties of sisal fiber-reinforced PLA biocomposites

Fiber content (Wt%)	Tensile Strength (MPa)	Tensile Modulus (GPa)	Flexural Strength (MPa)	Flexural Modulus (GPa)	Impact Strength (KJ/m²)	Elongation at break (Wt%)
0	64.5 ± 2.4	2.9 ± 0.10	109.6±8.3	3.1±0.2	2.97±0.45	1.2±0.4
5	66.8 ± 4.0	3.38 ± 0.30	120.3±7	4.6±0.3	3.28±0.3	1.3±0.35
10	69.6 ± 2.0	3.72 ± 0.60	125.5±9	5±0.5	3.56±0.4	1.8±0.53
15	70.8 ± 4.3	4.60 ± 0.20	135.1±7.4	5.6±0.1	3.87±0.34	2.1±0.69
20	70.9 ± 2.2	4.7 ± 0.25	136.5±9.3	5.7±0.3	5.64±0.24	2.3±0.23

25	69.7 ± 3.3	4.97 ± 0.30	135.4±10.6	5.8±0.25	4.98±0.46	1.89±0.59
30	68.7 ± 2.6	5.01 ± 0.14	134.5±9.5	6±0.24	4.96±0.54	1.75±0.48

The mechanical properties of PLA biocomposites reinforced with other biofibers are reported in Table 3 for comparison of the mechanical properties of biofiber-reinforced PLA biocomposites. Table 4 summarizes the thermal Properties of sisal fiber-reinforced PLA biocomposites As can be observed the tensile strength of PLA/30%SF is 69.3 MPa; this value is significantly higher than that of PLA with 30% flax reinforcement (54.15 MPa) and that of PLA with 30% Cordenka reinfocement(57.7 MPa) studied by Bax [18]. The PLA biocomposites reinforced with Moroccan sisal fibers in the current study showed good tensile strength (Table 3, Figure 1). The tensile strength of PLA biocomposites based on untreated and treated ramie fibers showed that shows a resistance lower than the strength of the composite based on Moroccan sisal fibers [34]..

Table 3 Comparison of the mechanical properties of PLA biocomposites based on bio-based fibers

Bio-based fibers /PLA	Fiber content [wt%]	Tensile strength [MPa]	Tensile modulus [GPa]	Flexural strength [MPa]	Flexural modulus [GPa]	Impact strength [kJ/m^2]	References
Ramie/PLA	30	16.15%	-	16.30%	-	28.57%	[35]
Hemp/PLA	30	2.2 %	70%	-	-	-	[37]
Abaca/PLA	30	17.46%	132%	13.76%	130%	150%	[43]
Sisal/PLA	30	6.5%	72.7%	22.7%	93.5%	67%	Current study
Sisal/PLA	20	9.8%	62%	24.5%	83.8%	89.8%	Current study

3.2.Differential scanning calorimetry (DSC)

The thermal properties of the PLA biocomposites were studied by differential scanning calorimetry. The DSC results are summarized in Table 3 and Figure 5. During the heating cycle, the glass transition temperature of the pure PLA was around 58 °C. Various amounts of sisal fibers in the PLA biocomposites did not significantly modify the glass transition temperature of the PLA. The highest T_g was measured in the case of PLA biocomposites reinforced by 20 wt% sisal fiber.

The diameter of sisal fibers did not have any effect on the mobility of the molecular chains of polylactic acid [31].

The melting enthalpy of the biocomposites was calculated in the second heating cycle (Figure 4). The maximum melting enthalpy of the PLA biocomposites was measured at 15 wt% of sisal fiber content. This maximum is attributed to the presence of crystallite forms in this biocomposite. At higher sisal fiber contents, the melting enthalpy is lower compared to pure PLA. The melting enthalpy of PLA/20%SF, PLA/25%SF and PLA/30%SF is 29.2%, 39.58% and 55.9% lower, respectively, than that of pure PLA.

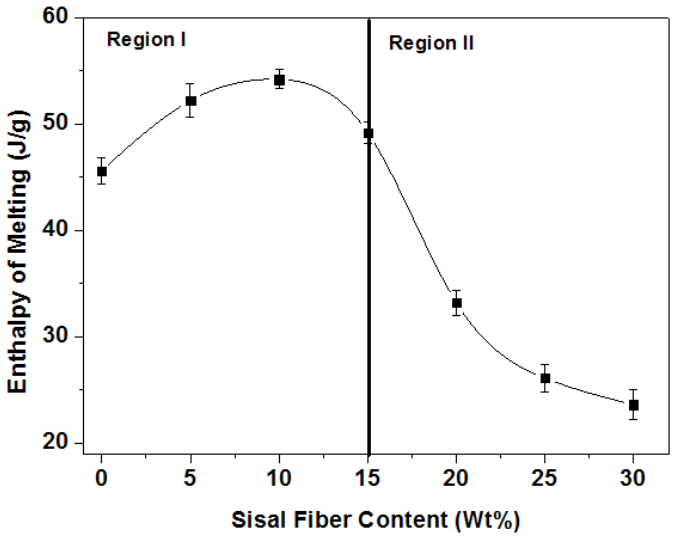

Figure 4. The crystal melting enthalpy of PLA biocomposites at different sisal fiber contents

Table 4 shows the thermal properties of the composites. The degree of crystallinity of the composites was improved by the sisal fiber reinforcement. The degree of crystallinity of the PLA biocomposites improved by increasing the weight fraction of the sisal fiber; the maximum was obtained with 10% sisal fiber content. The highest crystallinity of PLA biocomposites was 21.96% higher than that of pure PLA. This increase is due to the presence of nucleation sites initiating spherulite growth. The degree of crystallinity decreased with fiber contents higher than 10% because the growth of spherulites was limited by the available space between the fibers in the PLA.

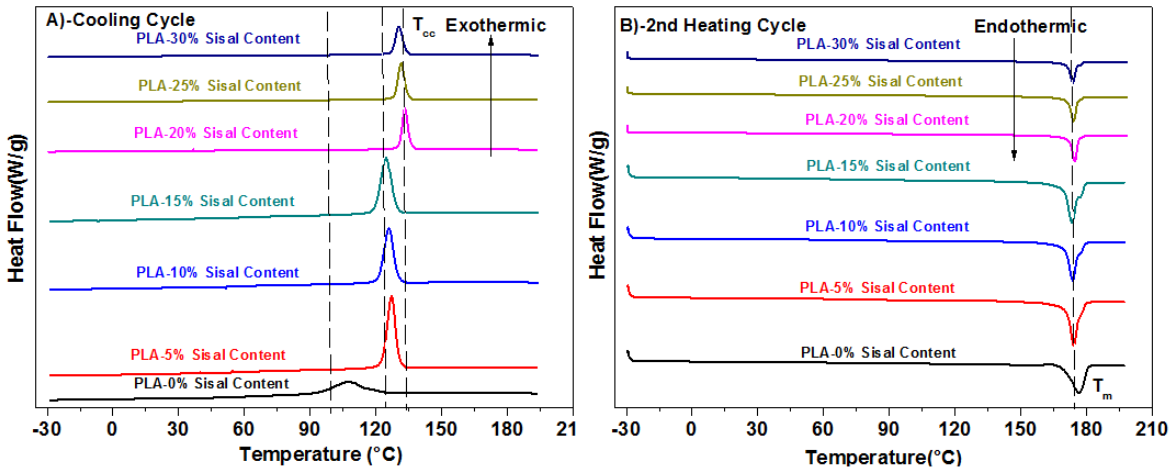

Figure 5 DSC thermograms of sisal fiber-reinforced PLA biocomposites

Table 4 Thermal Properties of sisal fiber-reinforced PLA biocomposites

Fiber content [wt%]	Glass transition temperature T_g [°C]	Cold crystallization temperature T_c [°C]	Cold crystallization enthalpy [J/g]	Melting temperature [°C]	Degree of crystallinity [%]
0	58.3	103.6	34.4	176.5	47.0
5	58.5	122.4	37.4	174.2	58.4
10	58.5	121.7	39.2	174.7	61.2

15	58.1	121.4	41.7	175.2	57.3
20	59.1	126.3	41.0	174.5	56.6
25	58.6	125.4	42.1	174.0	55.4
30	58.5	125.3	39.1	173.8	54.2

3.4. Thermogravimetric Analysis (TGA)

The thermal TGA curves of virgin PLA and the PLA biocomposites are shown in Figure 6 and Table 5 shows their thermal stability. The initial thermal degradation of PLA biocomposites starts before the initial thermal degradation of pure PLA, which can be attributed to the presence of moisture in sisal fibers. The thermal degradation temperatures of pure PLA, and 15%, 20%, 25% and 30% sisal fiber contents are 361 °C, 320 °C , 344°C , 331 °C and 341 °C, respectively. The addition of sisal fibers to PLA decreases the thermal degradation temperature. In general, natural fibers have less thermal stability than the pure matrix; it was reported that the addition of natural fibers will reduce the thermal stability of the biopolymer [34, 35].

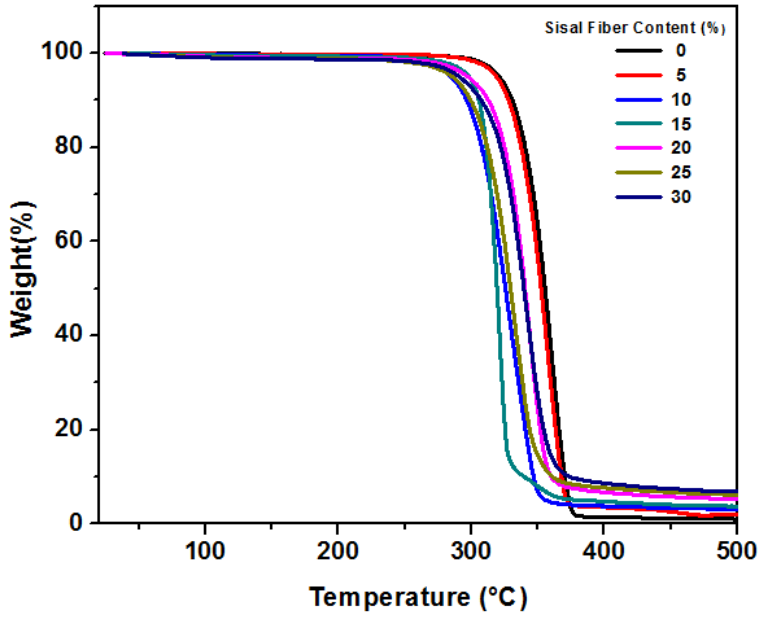

Figure 6 TGA curves of sisal fiber-reinforced PLA biocomposites

Table 5 Thermal stability of sisal fiber-reinforced PLA biocomposites

Fiber content [Wt%]	Thermal degradation temperature [°C]	Residual weight [%]	Temperature of residual weight [°C]
0	360.8	0.8	480
5	315.3	4.8	461
10	317.5	4.2	436
15	320.3	3.7	426
20	343.9	4.8	474
25	331.17	5.6	475

30	341.5	6.7	490

3.5. Dynamic Mechanical Analysis (DMA)

3.5.1. Analysis of the storage modulus of the biocomposites

The dynamic mechanical properties of the PLA biocomposites and the pure PLA in the temperature range from room temperature to 95 °C were investigated by DMA. The storage modulus curves of the composites are shown in Figure 7(a). In the glassy state, the addition of sisal fibers to PLA biocomposites lead to an increase in their storage modulus (E'_g), as indicated by the arrow in Figure 7(a). The storage modulus values of the pure PLA, PLA/15% SF, PLA/20%SF, PLA/25%SF and PLA/30%SF are 2718 MPa, 3430MPa, 3844MPa, 3779 MPa and 4857 MPa, respectively. The transition state of the PLA biocomposites between the glassy state and the rubbery state causes a decrease in the storage modulus.

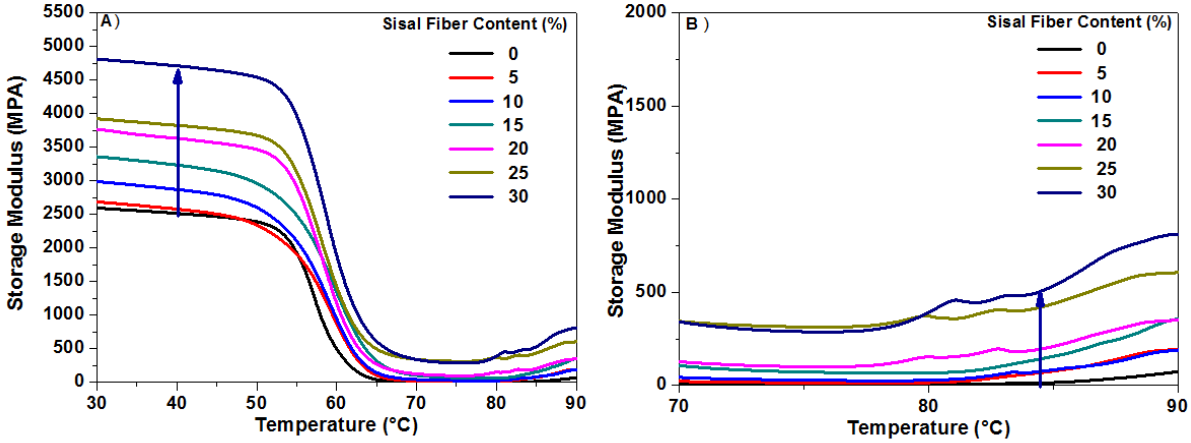

Figure 7 (a) Storage Modulus curves of the sisal fiber-reinforced PLA biocomposites in the temperature range from 30 °C to 90 °C, (b) Storage Modulus curves in the rubbery state in the temperature range from 70 °C to 90 °C.

In the rubbery state, the storage modulus curves in the temperature range from 70 °C to 90 °C can also be seen in Fig 7 (b) and show the impact of the sisal fiber. Thus, the addition of sisal fibers in PLA biocomposites lead to increase in the storage modulus (E'_r), as indicated by the arrow in Fig 7 (b). Therefore, the addition of sisal fibers to PLA biocomposites improves both storage modulus values (E'_g and E'_r) in the glassy and rubbery state. We will use these values in the following section to quantify the improvement. Adding natural fibers to PLA biocomposites enhance the storage modulus of PLA [34, 36].

3.5.2. Analysis of the reinforcement efficiency of sisal fiber

At the beginning, we evaluated the effectiveness constant of the reinforcement of sisal fibers in PLA biocomposites with (43). This expression was also used in previous studies to calculate the effectiveness constant of sisal fiber reinforcement in epoxy composites [43-44].

$$\epsilon = \frac{\left(\frac{E'_g}{E'_r}\right)_{Composite}}{\left(\frac{E'_g}{E'_r}\right)_{pure\ PLA}}, \quad (4)$$

where E'_g and E'_r are the storage moduli in the glassy and rubbery state, respectively.

It was reported that a smaller value of the coefficient (∈) indicates a better effectiveness of the reinforcement [43-44]. Gupta [44] showed that a sisal fiber content of 25% in epoxy composites has the highest reinforcement efficiency, as the coefficient (∈) is lowest here. Therefore, the authors concluded that the epoxy composite with a sisal fiber content of 25% has higher reinforcing power than with other amounts of sisal fiber reinforcement (15%, 20% and 30%). In our current study, eq. (4) was also used to calculate the effectiveness constant of sisal fiber reinforcement in PLA biocomposites.
Table 6 shows the effectiveness constant of reinforcement (∈) for sisal fibers in PLA biocomposites. According to the analysis [44], the effectiveness constant (∈) decreased from 1 to 0.06 as the amount of reinforcement increased from 0% to 30%, indicating that the best reinforcement efficiency is at 30 %.

Table 6. Effectiveness constant of sisal fiber reinforcement (∈) in PLA biocomposites

Sisal fiber content [wt%]	Storage modulus in the glassy state (E'_g) [MPa]	Temperature of E'_g [°C]	Storage Modulus in the rubbery state (E'_r) [MPa]	Temperature of E'_r [°C]	Effectiveness constant ∈ from (4)
0	2594	30.1	8.8	70.7	1
5	2690	30.0	20.5	70.4	0.44
10	2990	30.0	30.6	70.3	0.33
15	3359	30.1	78.01	70.1	0.14
20	3724	30.2	110.3	70.1	0.12
25	3766	30.1	116.2	70.1	0.11
30	4812	30.1	287.4	70.4	0.06

The value of the storage modulus of the composites the in glassy phase (E'_g) and the rubbery phase (E'_r) increased as sisal fiber content was increased from 0% to 30%. This behavior can also be seen from the storage modulus curves in Figure 7 (a) and (b). It seems that adding sisal fibers to PLA enhanced its mechanical properties. Therefore the effectiveness of the reinforcement is expected to increase. In addition, the storage modulus of the composites in the glassy phase (E'_g) and the rubbery phase (E'_r) showed a clear increase with the addition of the sisal fiber, as shown in Figure 7 (a) and (b). In this study, we tried to examine the change of storage modulus in both the in glassy state (E'_g) and the rubbery phase (E'_r) by increasing sisal fiber content, as shown in Figure 8. The effectiveness of the reinforcement of sisal fibers in PLA biocomposites exhibited a clear increase with increasing fiber content.

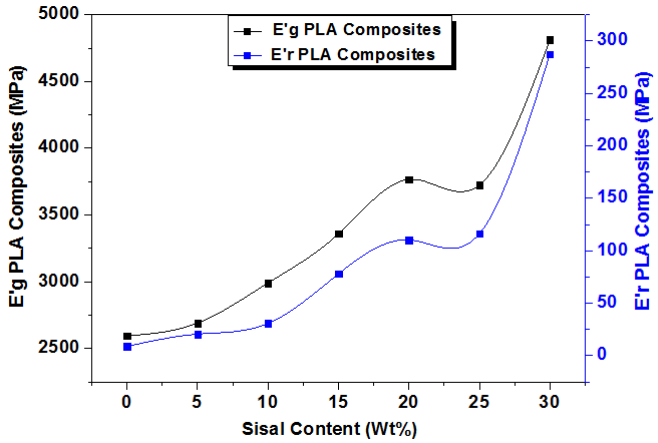

Figure 8 Storage modulus of PLA biocomposites in the glassy (E'_g) and the rubbery phase (E'_r)

In order to further investigate this behavior, we plotted the ratio of the storage modulus of the composites in the glassy state (E'_g) and the rubbery phase (E'_r) for the composite and PLA alone, against sisal fiber content as well as the effectiveness of reinforcement (Figure 9 (a) and (b)).

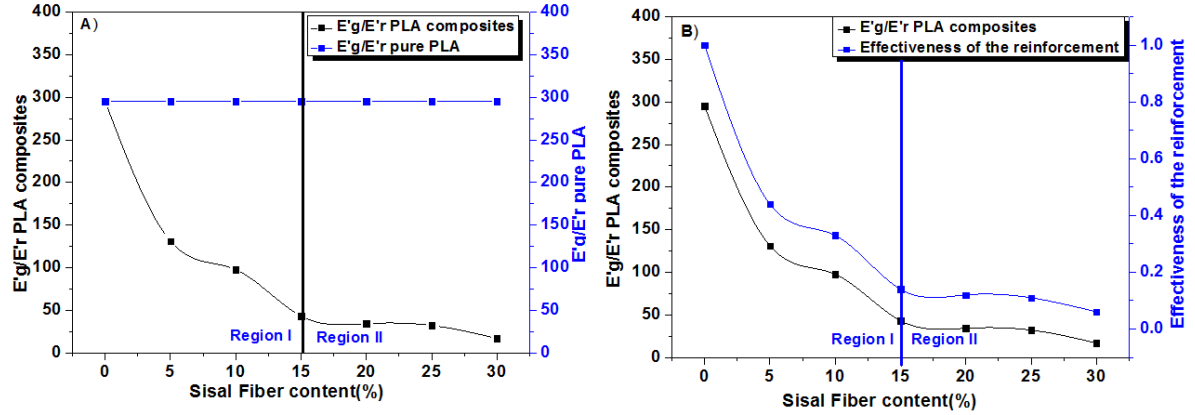

Figure 9 (a) Ratio of (E'_g) and (E'_r) of the biocomposites and pure PLA with different weight fractions of sisal fiber (b) Effectiveness of reinforcement (∈) using eq. (4)

From Figure 9, it is clear that the value of the effectiveness of reinforcement is less than 1, since the storage modulus in the vitreous and the rubber phase for the composite is lower than that of pure PLA, as demonstrated in Figure 9 (a). In order to understand why the effectiveness constant (∈) decreased with the increase of sisal fiber content, we have to examine both terms in the ratio given in eq. (4).

On the basis on our previous studies using the impedance spectroscopy method [45-47], we tried to find another, more accurate relationship between the effectiveness constant (∈) to and sisal fiber content. From electrical measurement, i.e. impedance spectroscopy, the inhibition efficiency IE% can be determined and it is usually used to highlight the effect of the polymer in preventing corrosion [48-50]. The inhibition efficiency (IE%) is expressed by the expression below (5):

$$\mathrm{IE}(\%) = \left(\frac{\mathrm{Rct}-\mathrm{R°ct}}{\mathrm{Rct}}\right) * 100, \quad (5)$$

where R^o_{ct} and R_{ct} are the charge transfer resistances without and with an inhibitor, respectively. It is important to note that the charge transfer resistance R_{ct} depends on the charge transfer between the electrolyte and the electrode with the addition of the polymer used as an inhibitor of corrosion. The above expression could very well reflect the change and the impact following the addition of the polymer used as an inhibitor of corrosion. The inhibition efficiency (IE%) usually increases as a function of polymer concentration. In this case, a new relationship given in eq (5) is proposed for the evaluation of the effectiveness constant of reinforcement (∈).

$$\in = \frac{\left(\frac{E'_r}{E'_g}\right)_{composite} - \left(\frac{E'_r}{E'_g}\right)_{pure\ PLA}}{\left(\frac{E'_r}{E'_g}\right)_{composite}} \quad (6)$$

The expression given in eq. (6) seems to be more convenient to evaluate the impact of the addition of sisal fiber in PLA and could describe the reinforcement efficiency (RE %) very well. It includes the use of parameters similar to the storage modulus in the glassy (E'_g) and the rubbery phase (E'_r) for composites and pure PLA. In addition, it could translate the change and the difference that occurred due the addition of the sisal fiber. However; the ratio (E'_g/E'_r) of the storage modulus in the glassy (E'_g) and the rubbery phase (E'r) used in eq. (4) was transformed to its inverse—(E'_r/E'_g).
Table 7 shows the effectiveness constant (∈) as well the both ratio of (E'g/E'r) and (E'r/E'g) for sisal fibers in PLA biocomposites using the proposed relationship (6).

Table 7 Effectiveness constant (∈) for sisal fiber-reinforced PLA biocomposites using the proposed relationship given in (5)

Sisal fiber content [wt%]	Storage modulus in the glassy state (E'g) [MPa]	Temperature of (E'g) [°C]	Storage Modulus in the rubbery state (E'r) [MPa]	Temperature of (E'r) [°C]	Effectiveness constant ∈ from (6)
0	2594	30.1	8.79	70.69	1
5	2690	30.0	20.52	70.40	0.44
10	2990	30.0	30.65	70.25	0.33
15	3360	30.1	78.01	70.12	0.14
20	3725	30.18	110.3	70.05	0.12
25	3767	30.14	116.2	70.14	0.11
30	4813	30.06	287.4	70.42	0.06

*: Ratio of E'g/E'r used to calculate the effectiveness constant (∈) in Eq. (4) [44].
**: Ratio of E'r/E'g used to calculate the effectiveness constant (∈) in Eq. (6) Current study.
***: Effectiveness constant (∈) using Eq. (6). Current study

From Table 7, it can be observed that the storage modulus in the glassy (E'g) and the rubbery phase (E'r) increase as sisal fiber content is increased, as shown in Table 6. However, the

ratio (E'g⁄ E'r) used eq. (4) to evaluate the effectiveness constant (∈) for sisal fiber–PLA biocomposites decreased. In contrast, the ratio (E'r⁄ E'g) showed a very clear increase when sisal fiber content increased. Consequently, the effectiveness constant (∈) calculated with Eq. (6) showed an increase as sisal fiber content increased. All these data were plotted in Figure 10 (a) and (b) in a similar way to Figure 9 (a) and (b) to better illustrate this behavior.

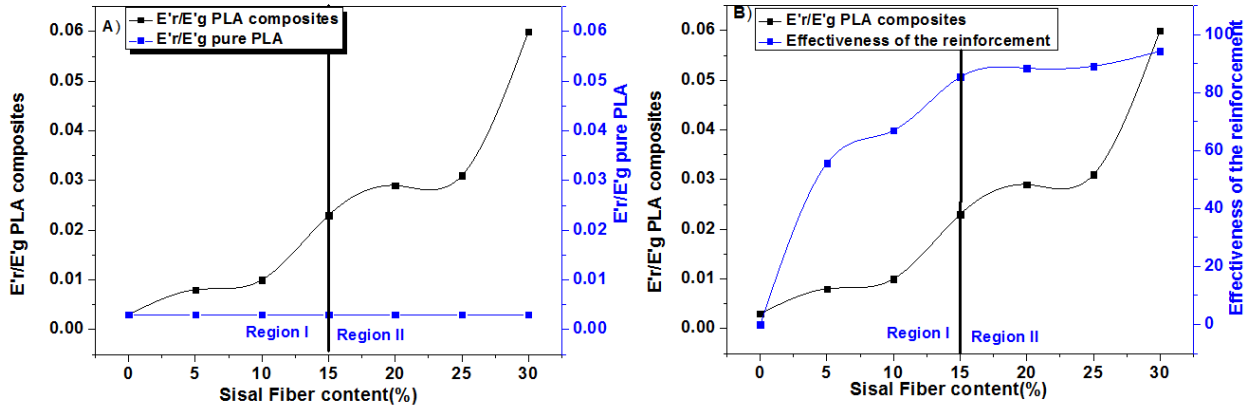

Figure 10 (a) Ratio of storage modulus in the glassy and rubbery phase of biocomposites and pure PLA with different weight fractions of sisal fiber (b) Effectiveness of the reinforcement ∈ calculated with (5)

Figure 9 (a) shows that E'r⁄E'g as a function of sisal fiber content showed a net increase, whereas E'r⁄E'g as a function of sisal fiber content for the PLA biocomposites does not change. The E'r⁄E'g curve for the composite is above that of pure PLA. Moreover, the effectiveness constant (∈) calculated with eq. (6) showed a clear increase when sisal fiber content increased and showed a similar trend to the E'r⁄E'g curve of the composite. Therefore, the new proposed relationship in eq. (6) can be very useful to evaluate the effectiveness rate of any kind of composite.

3.5.3. Analysis of the loss modulus of the biocomposites

The loss modulus of the composites was investigated with a universal analyzer (Figure 11(a)). The loss modulus of the samples improved as the weight fraction of sisal fibers increased in PLA biocomposites at a temperature below the glass transition temperature. The glass transition temperature of polylactic acid is still close to 60 °C after the addition of sisal fibers. The loss modulus in PLA biocomposites was maximum at 30% sisal fiber content. Shakoor et al [37] examined the impact of hemp fiber as reinforcement in polylactic acid on the loss modulus of the biocomposite. His results were similar to the results of the current study. The glass transition temperature (T_g) of PLA biocomposites measured from the loss modulus curve are presented in Table 7. The highest T_g in the PLA biocomposites was measured at a sisal fiber content of 20%.

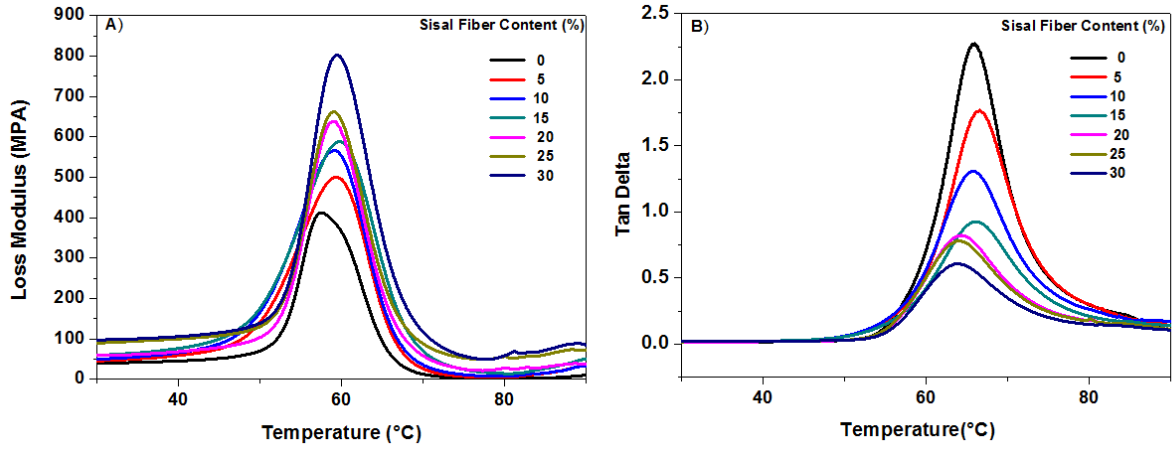

Figure 11 (a-b) Loss Modulus and Tan Delta of sisal fiber-reinforced PLA biocomposites

Figure 11 (b) illustrates the tan delta of PLA biocomposites. The pure PLA has a higher tan delta than the sisal fiber–PLA composites. The tan delta of PLA biocomposites decreased as the weight fraction of sisal fibers was increased. It is due to the low damping capacity of sisal fibers. The effect of hemp fibers is similar to that of sisal fibers (current study) on the dynamic mechanical properties of PLA biocomposites [51]. The glass transition temperature (T_g) of PLA biocomposites given by the tan delta curve is higher than the glass transition temperature given by the loss modulus curve (Table 8).

Table 8 Glass transition temperature (T_g) of sisal fiber-reinforced PLA biocomposites

Fiber content [wt%]	T_g (Loss modulus Figure 10 (a) [°C]	T_g (tan delta Figure 10 (b) [°C]
0	57.8	65. 8
5	59.3	65.9
10	59.0	65.5
15	59.5	65.8
20	59.6	66.1
25	59.1	64.1
30	59.3	63.9

3.6. SEM microstructure of biocomposites

The surface structures of PLA biocomposites are illustrated in Figure 12. Increasing the amount of sisal fibers allows for their uniform distribution in the PLA matrix. A low reinforcement content results in poor adhesion between the sisal fibers and the PLA matrix. Adhesion impacts the mechanical properties of PLA biocomposites. The optimal sisal fiber content was 20%, which resulted in a good distribution of the fibers in the PLA biocomposites (Figure 12 C)). A further increase in sisal fiber content leads to interaction between the fibers, and between the fibers and the extruder wall, which leads to fiber fragmentation along the composite test specimens. The SEM micrographs show the fact that fiber tearing increased with an increase in sisal fiber content [52]. The relationship between mechanical properties and sisal fiber content is non-linear, which is shown by the saturation of the surface of the PLA above 20% sisal fiber content, and which can be well identified in the SEM images.

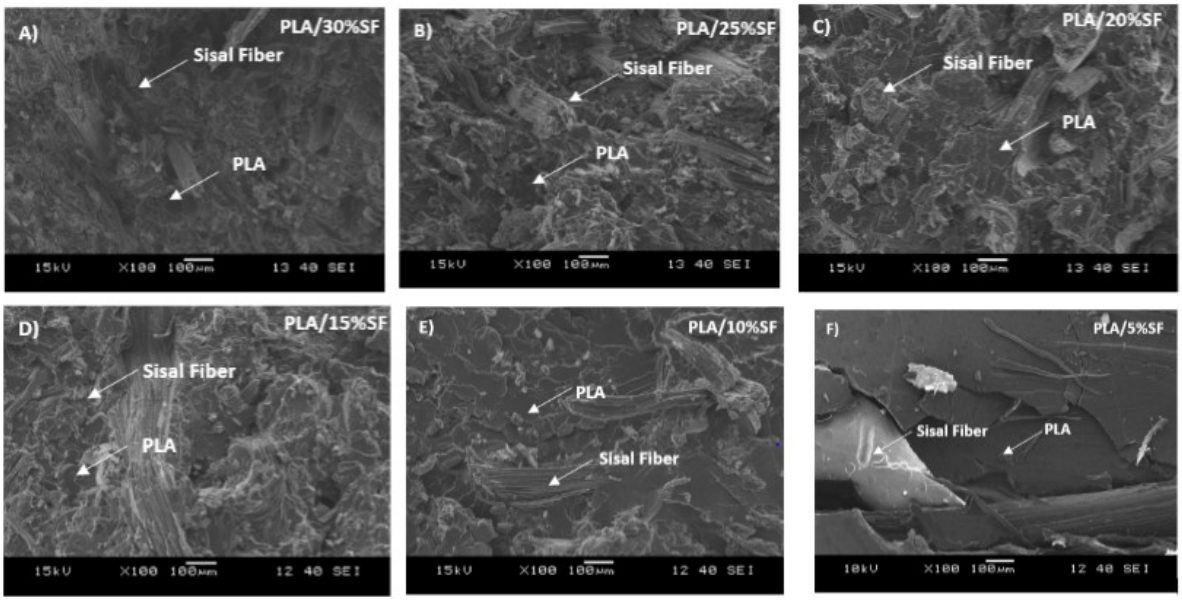

Figure 12 SEM images of fracture surface of sisal fiber-reinforced PLA biocomposites A) SEM image of PLA/30% sisal fiber composites, B) SEM image of PLA/25% sisal fiber composites ,C) SEM image of PLA/25% sisal fiber composites, D) SEM image of PLA/15 % sisal fiber composites , E) SEM image of PLA/10% sisal fiber composites, F) SEM image of PLA/5% sisal fiber composites.

Conclusion:

The aim of this study was to investigate the effect of Moroccan sisal fiber reinforcement on the properties of PLA biocomposites. Fiber content was varied between 15% and 30% while data for smaller fiber contents were taken from our previous study. The PLA and sisal fiber were compounded by twin-strew extrusion, and then composite samples were produced by injection molding.

An increase in sisal fiber content in the PLA biocomposites gradually improved tensile strength, tensile modulus, and flexural and impact properties. The increase of fiber content also improved Charpy impact properties. Hence, the PLA biocomposites showed high mechanical performance. The dynamic mechanical (DMA) and the differential scanning calorimetry (DSC) analysis proved that increasing sisal fiber content of the PLA biocomposites did not significantly affect the glass transition temperature, but decreased the tan delta at glass transition. The crystallinity of the PLA biopolymer increased significantly when Moroccan sisal fibers were added, which shows the role of this fiber as a nucleating agent.

Considering all the mechanical properties tested, we can conclude that at 20% fiber content mechanical properties were the best. Also, we proposed a new formula to evaluate the effectiveness rate of the composite due to the addition of sisal fiber.

Acknowledgements

The current research was supported by the National Science Centre for Scientific and Technical Research and the Technical Research Development and Innovation Office (TÉT_16-1-2016-0114. Hungary). This paper was also supported by the János Bolyai Research Scholarship of the Hungarian Academy of Sciences (MTA), the by the ÚNKP-20-5 New National Excellence Program of the Ministry for Innovation and Technology (Kolos Molnár).

References

[1] M. K. S . Sai , Int. J. Latest Trends Eng. Technol. **2016** , 6(3),129.

[2] M. Delgado,M. Felix,C. Bengoechea, Ind. Crop. Prod . **2018**, 128, 401 . https://doi.org/10. 1016/ j.indcrop.2018.09.013.

[3] G. Bogoeva-Gaceva,M. Avella,M. Malinconico,A. Buzarovska,A. Grozdanov,G. Gentile, M.E. Errico, Polym. Compos. **2007**, 28(1), 98. https://doi.org/10.1002/pc.20270.

[4] A.C .Corbin, B. Sala, D. Soulat,M. Ferreira, A. R. Labanieh, V. Placet,J. Compos. Mater . **2020**, 0021998320954230.https://doi.org/10.1177/0021998320954230.

[5] Y. He,Y. Zhou,H.Wu, Z.Bai, C. Chen, X. Chen, S. Qin, J. Guo, Mater. Chem. Phys. **2020**, 123247. https://doi.org/10.1016/j.matchemphys.2020.123247.

[6] D. Pantaloni, A. L. Rudolph, D. U.Shah, C.Baley, A. Bourmaud ,Compos. Sci. Technol. **2020**, 108529.https://doi.org/10.1016/j.compscitech.2020.108529.

[7] S. M.Darshan,B. Suresha, Mater. Today. **2020**, https://doi.org/ 10.1016j.matpr. 2020.07. 618.

[8] V.Carvelli, A.Veljkovic, H. Nguyen, A. Adediran, P. Kinnunen, N. Ranjbar, M. Illikainen, Cem Concr Compos.**2020**, 114, 103805.https://doi.org/10.1016/j.cemconcomp.2020.103805.

[9] C. Chen, Y. Yang, Y. Zhou, C. Xue, X. Chen, H. Wu, L. Sui, X . Li, J. Clean. Prod.**2020**, 121572. https://doi.org/10.1016/j.jclepro.2020.121572.

[10] Y. Wu, C. Xia, L.Cai,A.C Garcia, SQ. Shi, J. Clean. Prod .**2018**, 184 ,92 . https://doi.org/10. 1016 /j.jclepro.2018.02.257.

[11] N. D. O. R. Maciel, J. B. Ferreira, J. da Silva Vieira, C. G. D. Ribeiro, F. P. D. Lopes, F.M. Margem, S. N. Monteiro,C. M. F. Vieira, L. C. daSilva, J. Mater. Sci. Technol. **2018**, 7(4), 561-565. https://doi.org/10.1016/j.jmrt.2018.03.009.

[12] K. L. Pickering, M. A. Efendy, T. M. Le, Compos .Part A Appl. Sci. Manuf. **2016** ,8 3 ,98 .https://doi.org/10.1016/j.compositesa.2015.08.038.

[13] A. Rubio-López, J. Artero-Guerrero, J. Pernas-Sánchez,C. Santiuste, Compression after impact of flax/PLA biodegradable composites, Polym. Test. **2017**, 59, 127. https://doi.org/ 10.1016 /j.polymertesting.2017.01.025.

[14] M. U.Wahit, N. I. Akos,W. A. Laftah, Polym. Compos. **2012**,33(7), 1045.https:// doi . org/10.1002/pc.22249.

[15] S. M.Lee ,D. Cho,W.H. Park, S. G.Lee, S. O. Han , L. T. Drzal, Compos. Sci. Technol. **2005**, 65(3-4) ,647.https://doi.org/10.1016/j.compscitech.2004.09.023.

[16] E. V.Torres-Tello,J.R. Robledo-Ortíz, Y. González-García,A.A. Pérez-Fonseca, C.F. Jasso-Gastinel,E. Mendizábal, Ind. Crop. Prod.**2017**,99,117.https://doi.org/ 10. 1016 / j . indcrop.2017.01.035.

[17] F.Z .Arrakhiz,M. El Achaby,M. Malha,M.O. Bensalah,O. Fassi-Fehri,R. Bouhfid, R. Qaiss, Mater. Des. **2013**,43, 200.https://doi.org/10.1016/j.matdes.2012.06.056.
[18] B. Bax, J. Müssig, Compos. Sci. Technol. **2008**, 68(7-8), 1601. https://doi.org/ 10. 1016 /j.compscitech.2008.01.004.
[19] R. Hu, J. K. Lim, J. Compos. Mater. **2007**, 41(13) , 1655. https://doi.org/ 10.1177 /00 2 1998306069878.
[20] K. Oksman, M. Skrifvars , JF. Selin, Compos. Sci. Technol. **2003**, 63: 1317–1324. https://doi.org/ 10.1016/S0266-3538(03)00103-9.
[21] D.Placketta, TL. Andersen , WB. Pedersenc , L.Nielsenc, Compos. Sci. Technol.**2003**, 63: 1287–1296.https://doi.org/10.1016/S0266-3538(03)00100-3.
[22] G.Gamon,P. Evon, L. Rigal, Ind. Crops. Prod.**2013**, 46,173.https://doi.org/ 10 . 1016 / j . indcrop.2013.01.026.
[23] S. Cheng,K.T. Lau,T. Liu,Y. Zhao, P.M. Lam,Y. Yin,Compos.B. Eng.**2009**,40(7), 650. https://doi.org/10.1016/j.compositesb.2009.04.011
[24] Y. Li,Y.W. Mai, L. Ye, Compos. Sci. Technol.**2000**, 60 (11), 2037. https://doi.org/ 10 . 1016/S0266-3538(00)00101-9.
[25] M. Sood , D. Deepak,V. K. Gupta ,Mater. Today. **2018**, 5(2),5673- 5678. https://doi.org /10. 1016/ j.matpr.2017.12.161.
[26] Z. Sun , W. Mingming , Ind. Crops. Prod.**2019**, 137, 89-97.https://doi.org/10.1016 /j.indcrop.2019.05.021.
[27] C. Ngaowthong, M. Borůvka, L. Běhálek, P .Lenfeld, M . Švec, R. Dangtungee,S . Siengchin, S . M. Rangappa, J . Parameswaranpillai, Waste. Manage. **2019** , 97, 71-81.https://doi.org/10.1016/j.wasman.2019.07.038.
[28] J.D. Badia,T. Kittikorn, E. Strömberg, L. Santonja-Blasco,Polym. Degrad. Stab.**2014**,108,166.https://doi.org/10.1016/j.polymdegradstab.2014.04.012.
[29] J. El-Hilaly,M. Hmammouchi,B. Lyoussi, J. Ethnopharmacol. **2003** ,86(2-3), 149. https://doi.org/10.1016/S0378-8741(03)00012-6.
[30] M. Fennane, M. Rejdali, Aromatic and medicinal plants of Morocco: richness. diversity and threats. Bulletin de l'Institut Scientifique, Rabat. Section Sciences de la Vie.**2016**.38.
[31] Z. Samouh, K. Molnar, F. Boussu, O. Cherkaoui, R. El Moznine,Polym. Adv.Technol. **2019**, 30(3),529. https://doi.org/10.1002/pat.4488.
[32] S. Fehri,P.Cinelli, M-B. Coltelli, I.Anguillesi, A. Lazzeri,Int. J. Chem. Eng.Appl. **2016**, 7(2),85.https://doi.org/ 10.7763/IJCEA.2016.V7.548.
[33] A. K. Mohanty, M. Misra, L.T. Drzal, Natural fibers. biopolymers. and biocomposites. CRC press.Taylor & Francis Group.Boca Raton , United States, 2005.
[34] T. Yu , J. Ren,S. Li, H.Yuan, Y. Li, Compos. Part A Appl. Sci. **2010**, 41(4), 499. https://doi.org/10.1016/j.compositesa.2009.12.006.
[35] M.S. Huda,L.T. Drzal, M. Misra, A.K. Mohanty, J. Appl. Polym. Sci.**2006**,102(5), 4856-4869. https://doi.org/10.1002/app.24829.
[36] R.S. Darsan, B .S.J .Retnam, M. Sivapragash, I . J . M . E . T.**2018**, 9(11),779.http://www.iaeme.com/ijmet/issues.asp?JType=IJMET&VType=9&IType=11.
[37] A. Shakoor, R. Muhammad,N.L. Thomas,V.V. Silberschmidt, In Journal of Physics: Conference Series (Vol. 451. No. 1. p. 012010) **2013** IOP Publishing.

[38] A. Pappu, K.L. Pickering, V.K. Thakur, Ind. Crops. Prod. **2019**, 137, 260. https://doi.org/ 10.1016 /j.indcrop.2019.05.040.
[39] S. S .Munawar,K. Umemura,S. Kawai, J. Wood. Sci.**2007**, 53(2) ,108 . https://doi.org/ 10 .1007/s10086-006-0836-x.
[40] J.T.Kim, A.N. Netravali, Compos. Part A Appl. Sci. Manuf.**2010**, 41(9), 1245. https://doi.org/10.1016/j.compositesa.2010.05.007.
[41] T.J. Bessell, S.M. Mutuli,J. Mater. Sci. Let. **1982** ,1(6), 244. http://link.springer. com/ article/10.1007%2FBF00727846?LI=true#page-1.
[42] F. de Andrade Silva,N. Chawla, R. D. de Toledo Filho, Compos. Sci. Tech.**2008**,68(15-16), 3438.https://doi.org/10.1016/j.compscitech.2008.10.001.
[43] A.K. Bledzki, A. Jaszkiewicz, D. Scherzer, Compos. Part A Appl. Sci. Manuf . **2009**, 40(4), 404.https://doi.org/10.1016/j.compositesa.2009.01.002.
[44] M.K .Gupta, R.K .Srivastava, Mater. Des.**2015**,41(3),65.https://doi.org/235-241.10. 15224/ 978-1-63248-072-9-52.
[45] A. Mortadi, A. Elmelouky, M. Chahbi, N. Ghyati, S. Zaim, O.Cherkaoui, R.El Moznine, Acta A Mol. Biomol. Spectrosc. **2020**,224,117437.https://doi.org/10.1016/j.saa.2019.117437.
[46] A. Mortadi, E.G Chahid, A. Elmelouky, M. Chahbi, N .Ghyati, S. Zaim, O. Cherkaoui,R . El Moznine,Water. Resour. Res.**2020**, 100130.https://doi.org/10.1016/j.saa.2019.117437.
[47] A. Mortadi, A. Elmelouky, E. G. Chahid,R. Essajai, H. Naserllah, M. Chahbi, O.Cherkaoui, R. El Moznine,J. Environ. Chem. Eng.**2020**, 8(3), 103764.https://doi.org/ 10.1016/j.jece.2020.103764.
[48] T. Benabbouha, M. Siniti, H. El Attari, K .Chefira, F .Chibi, R. Nmila,H. Rchid, Journal of Bio-and Tribo-Corrosion. **2018**, 4(3),39.https://doi.org/10.1007/s40735-018-0161-0.
[49] A. Popova, E. Sokolova, S. Raicheva, M. Christov, Corros. Sci. **2003** ,45,33. https://doi. org/10.1016/S0010-938X(02)00072-0.
[50] A.A. Gürten, H. Keleş, E .Bayol, F. Kandemirli,J. Ind. Eng. Chem. **2015**, 27,68. https:// doi.org/10.1016/j.jiec.2014.11.046.
[51] H.O. Maurya, M.K. Gupta, R.K. Srivastava, H. Singh,Mater. Today.**2015**, 2(4-5), 1347. https://doi.org/10.1016/j.matpr.2015.07.053.
[52] M.A. Sawpan, K.L. Pickering, A. Fernyhough,Compos. Part A Appl. Sci. Manuf. **2011**, 42(3),310.https://doi.org/10.1016/j.compositesa.2010.12.004.

Figure Captions:

Figure 1. Tensile properties of sisal fiber-reinforced PLA biocomposites. (a) Curves (b) Histogram

Figure 2. Flexural properties of sisal fiber-reinforced PLA biocomposites. (a) Curves (b) Histogram

Figure 3. Impact properties of sisal fiber-reinforced PLA biocomposites. (a) Curves (b) Histogram

Figure 4. The enthalpy of melting of PLA biocomposites at different sisal fiber contents

Figure 5. DSC thermograms of sisal fiber-reinforced PLA biocomposites

Figure 6. TGA curves of sisal fiber-reinforced PLA biocomposites

Figure 7. (a) Storage modulus curves of the sisal fiber-reinforced PLA biocomposites in the temperature range from 30 °C to 90 °C (b) Storage Modulus curves in the rubbery state in the temperature range from 70 °C to 90 °C.

Figure 8. Storage modulus of the PLA biocomposites in the glassy (E'_g) and the rubbery

phase (E'_r)

Figure 9 (a) Ratio of (E'_g) and (E'_r) of the biocomposites and pure PLA with different weight fractions of sisal fiber (b) Effectiveness of reinforcement ($\in$) using eq. (4)

Figure 10 (a) Ratio of storage modulus in the glassy and rubbery phase of biocomposites and pure PLA with different weight fractions of sisal fiber (b) Effectiveness of reinforcement $\in$ using eq. (6)

Figure 11 Loss Modulus and Tan Delta of sisal fiber-reinforced PLA biocomposites

Figure 12 SEM images of sisal fiber-reinforced PLA biocomposites